Neurobiology of Disease 124 (2019) 311–321

Contents lists available at ScienceDirect

Neurobiology of Disease

journal homepage: www.elsevier.com/locate/ynbdi

Human Tau isoform-specific presynaptic deficits in a Drosophila Central Nervous System circuit

Dimitrios Kadas[a], Katerina Papanikolopoulou[b,1], Sofia Xirou[a,1], Christos Consoulas[a,*], Efthimios M.C. Skoulakis[b,*]

[a] Laboratory of Experimental Physiology, National and Kapodistrian University of Athens, 11527 Athens, Greece
[b] Division of Neuroscience, Biomedical Sciences Research Centre "Alexander Fleming", 34 Fleming str, Vari 16672, Greece

A B S T R A C T

Accumulation of normal or mutant human Tau isoforms in Central Nervous System (CNS) neurons of vertebrate and invertebrate models underlies pathologies ranging from behavioral deficits to neurodegeneration that broadly recapitulate human Tauopathies. Although some functional differences have begun to emerge, it is still largely unclear whether normal and mutant Tau isoforms induce differential effects on the synaptic physiology of CNS neurons. We use the oligosynaptic Giant Fiber System in the adult Drosophila CNS to address this question and reveal that 3R and 4R isoforms affect distinct synaptic parameters. Whereas 0N3R increased failure rate upon high frequency stimulation, 0N4R compromised stimulus conduction and response speed at a specific cholinergic synapse in an age-dependent manner. In contrast, accumulation of the R406W mutant of 0N4R induced mild, age-dependent conduction velocity defects. Because 0N4R and its mutant isoform are expressed equivalently, this demonstrates that the defects are not merely consequent of exogenous human Tau accumulation and suggests distinct functional properties of 3R and 4R isoforms in cholinergic presynapses.

1. Introduction

Tauopathies encompassing > 20 distinct clinicopathological conditions are adult onset neurodegenerative dementias including the widespread Alzheimer's disease (AD) among others (Lee et al., 2001). Although they present overlapping pathologies affecting particular brain areas differentially (Delacourte, 2005), the manifestations of these dementias can be broadly grouped into ones linked to neuronal dysfunction and others to neurotoxicity, with a potential temporal progression from the former to the latter (Lee et al., 2001; Papanikolopoulou and Skoulakis, 2015). They involve dysregulation or malfunction of the neuronal protein Tau, which presents 6 isoforms in the adult human brain due to alternative splicing of a single transcript into species that incorporate 3 (3R) or 4 (4R) conserved repeats and inclusion (1 N or 2 N) or absence (0 N) of particular aminoterminal sequences (Delacourte, 2005; Sergeant et al., 2005). The functional significance of the different Tau isoforms has not been fully elucidated yet, but tissue specific differences in their distribution suggest that they are likely to have distinct physiological functions (Avila et al., 2004; Sergeant et al., 2005). Although multiple functions within different neuronal types are emerging (Sotiropoulos et al., 2017), Tau is thought to bind axonal microtubules via the repeats and hence potentially regulate intraneuronal transport (Delacourte, 2005; Sergeant et al., 2005).

The etiology of Tauopathies, especially sporadic ones is unclear, but involves differential aggregate formation containing hyperphosphorylated 3R or 4R isoforms, while FTDP-17 is associated with actual mutations in the Tau gene (Goedert, 2005). The pathologies characterizing the distinct Tauopathies appear correlated with the isoform-specific constitution of aggregates (Buee et al., 2000; Lee et al., 2001; Sergeant et al., 2005). Therefore, elucidating isoform specific molecular and physiological differences is essential to understand their apparent differential involvement in different Tauopathies and contribution to neuronal dysfunction and toxicity.

Animal models have been generated to investigate the relationship of mutant and normal Tau accumulation, hyperphosphorylation and misregulation and the molecular mechanisms requisite for the formation and maintenance of these pathogenic species (Lee et al., 2005; Papanikolopoulou and Skoulakis, 2011; Sang and Jackson, 2005). Drosophila figures prominently among these models and has been instrumental in discoveries of novel molecular mechanisms and pathways leading to pathogenicity and dysfunction (Crowther et al., 2006; Gotz et al., 2007; Marsh and Thompson, 2004). Most of the work in Drosophila as in other models focused on the pathogenicity of human wild type and mutant Tau with emphasis on neurodegeneration and lately on dysfunction manifested as learning and memory (Kosmidis et al., 2010;

* Corresponding authors.
E-mail addresses: cconsoul@med.uoa.gr (C. Consoulas), skoulakis@fleming.gr (E.M.C. Skoulakis).
[1] equal contribution.

https://doi.org/10.1016/j.nbd.2018.12.004
Received 27 June 2018; Received in revised form 19 November 2018; Accepted 6 December 2018
Available online 08 December 2018
0969-9961/

Papanikolopoulou and Skoulakis, 2011; Papanikolopoulou and Skoulakis, 2015) and mobility deficits (Mudher et al., 2008; Sealey et al., 2017) among others. Interestingly, differences in the toxicity of wild type and FTDP-17-linked mutant Tau expressed in the Drosophila CNS (Kosmidis et al., 2010) and recently among different FTDP-17-linked mutations (Bardai et al., 2018) have been reported. Importantly, a recent study was the first to systematically compare the toxicity and dysfunction of 3R and 4R isoforms in distinct tissues and life stages of Drosophila (Sealey et al., 2017). These isoforms presented distinct phosphorylation patterns, the 3R isoform caused stronger axonal transport defects, locomotor impairments and a shorter lifespan than the 4R isoform. In contrast, accumulation of the 4R isoform yielded more profound neurodegeneration and independent of that neurotoxicity phenotype, deficits in learning and memory, which were absent in animals expressing 3R. These differential effects suggest differences in isoform biology and pathological potential (Sealey et al., 2017).

However, little is known to date of the effects of human Tau isoform-specific accumulation on the physiology and signal conduction properties of Central Nervous System (CNS) neurons in vivo. To address this, we capitalized on the anatomically and physiologically well-characterized Giant Fiber System (GFS), which mediates the escape reflex in Drosophila (Allen et al., 2006). The reflex is activated by a predator, or predator-mimicking stimuli and results in jump and flight initiation (Hammond and O'Shea, 2007; Trimarchi and Schneiderman, 1993). This well-defined oligo-synaptic neuronal circuit of the fly CNS is readily accessible electrophysiologically (Engel and Wu, 1992; Kadas et al., 2012; Tanouye and Wyman, 1980). Furthermore, different parts of the circuit can be targeted preferentially through the GAL4-UAS system. This permits isolated investigation of cholinergic from glutamatergic neurotransmission and the propagation of action potentials in axons of distinct well-defined neurons. Therefore, to establish a facile system to investigate the effects of human Tau (hTau) accumulation on the electrophysiological properties of the CNS, we targeted its expression in GFS neurons and assessed its effects on the performance of the circuit as a function of expressed isoform and age.

2. Materials and methods

2.1. Drosophila strains and culture

Flies were raised and aged on standard flour-yeast-agar medium at 24 °C in a humidified incubator. The following fly strains were used: The genetic background of all drivers and transgenes is w^{1118} into which all transgenes were introduced by repeated backcrosses for at least 6 generations. UAS-0N4R and UAS-0N4R^{R406W} were a kind gift of M. Feany (Wittmann et al., 2001), while 0N3R was provided by A. Mudher (Sealey et al., 2017). OK307 Gal4 is preferentially expressed in the GFS (Allen et al., 1998; Kadas et al., 2012). The GF-split Gal4 line [7A04-p65ADZP(attp40); 68A06-ZpGdbd(attpZ)] described previously (von Reyn et al., 2014) drives expression exclusively in Giant Fiber (GF) interneurons. Finally, the motor neuron-specific Gal4 line c380 (Boerner and Duch, 2010), which excludes their cholinergic component by constitutively expressing ChaGal80 has been described before (Duch et al., 2008; Ryglewski et al., 2014; Sanyal et al., 2003). Controls were generated by crossing the abovementioned drivers and transgenes to w^{1118}.

Cohorts of flies expressing the hTau transgenes under a particular driver and cognate controls were raised and aged concurrently. Male and female flies were used and for aging they were transferred to new vials every 3 days.

2.2. GF circuit analysis

Flies were anesthetized briefly with CO_2 or by cooling on ice, glued to a thin metal wire attached to the neck with cyanoacrylate adhesive and allowed to recover from anaesthesia for 30 min to 1 h. To stimulate electrically the GF neurons a pair of uninsulated, tungsten electrodes was used to penetrate the eyes. A similar electrode was used to record from the DLM (fibers 5 and 6) and TTM. A fourth tungsten reference electrode was placed into the scutellum or the abdomen (Allen et al., 2000; Engel and Wu, 1992; Kadas et al., 2012; Tanouye and Wyman, 1980). Brain stimulation was performed by delivering stimuli (0.15 ms in duration) with a Grass S88 stimulator (Quincy, Mass. U.S.A.), while DLM or TTM muscle action potentials were acquired in the 300 Hz to 10KHz frequency range and amplified 100× by a differential AC amplifier (A-M systems model 1700). Data were digitized with an analogue to digital converter (Digidata 1200, Axon Instruments) and without filtering were analysed and displayed with Clampex 8.1 version software (Axon Instruments).

2.3. Western blots

Single adult female flies (head + thorax) 1–3 days post-eclosion were homogenized in 1× Laemmli buffer (50mMTris pH 6.8, 100 mM DTT, 5% 2-mercaptoethanol, 2% SDS, 10% glycerol and 0,01% bromophenol blue). The lysates were boiled for 5 min at 95 °C, centrifuged at 10000 ×*g* for 5 min and separated by SDS-PAGE. Proteins were transferred to a PVDF membrane at 120 V for 80 min and probed with the monoclonal anti human Tau antibody 5A6 (Developmental Studies Hybridoma Bank) at 1:3000 and the monoclonal anti Drosophila Syntaxin 1A (Syx) antibody (8C3, Developmental Studies Hybridoma Bank) at 1:2000. Anti-mouse HRP-conjugated antibody was applied at 1:5000 and proteins were visualized with chemiluminescence (ECL Plus, Amersham). Signals were measured with Biorad's Molecular Imager Chemidoc™ XRS + and quantified with the Image Lab™ software. Results were plotted as means ± SEM from $n = 5$. To compare expression levels of transgenes under OK307-Gal4 driver between aged flies, animals were kept at 25C for 30 and 45 days.

2.4. Statistics

Statistics were performed with GraphPad Prism 6.00 for Windows (La Jolla California USA, www.graphpad.com). Data were tested for normality (D'Agostino & Pearson omnibus normality test) and Ordinary One way ANOVA with posthoc analysis (Dunnett's multiple comparisons test, alpha 0.05) was used to compare between multiple pairs. Data were presented as means and SEM, and significance levels were defined as $^{*}p < 0.05$; ** $p < 0.01$, $^{***}p < 0.001$ and **** $p < 0.0001$.

3. Results

The two bilaterally symmetrical giant fiber (GF) interneurons receive inputs from the optic lobe and send their axons from the brain, through the cervical connective, to the thoracic ganglion (Fig. 1A). In the mesothoracic neuromere, each GF axon makes electro-chemical synapses with two ipsilateral neurons. The peripherally synapsing interneuron (PSI; Fig. 1A) and the tergotrochanteral muscle motor neuron (TTMn; Fig. 2A). The PSI axon projects to the opposite side of the ganglion, enters the contralateral posterior dorsal mesothoracic nerve (PDMN) and forms therein cholinergic connections with the axons of four motor neurons (MN1-4; not shown), which terminate in the corresponding dorsal longitudinal flight muscles 1-4 (DLM1-4; not shown), and the axon of motoneuron 5 (MN5), known to innervate the most dorsal longitudinal flight muscles 5-6 (DLM5-6; Fig. 1A) (Allen et al., 2006). In contrast, the TTMn outputs directly via glutamatergic synapses onto the tergotrochanteral (jump) muscle (TTM- Fig. 2A). Therefore, recording muscle action potentials exclusively from DLM5–6 upon GF stimulation assesses the activity of the tri-neuronal pathway consisting of GF, PSI, and MN5 (Fig. 1A), whereas recording from the TTM reports activity of the GF-TTMn bi-neuronal circuit (Fig. 2A).

Estimation of the time between GF activation and muscle response

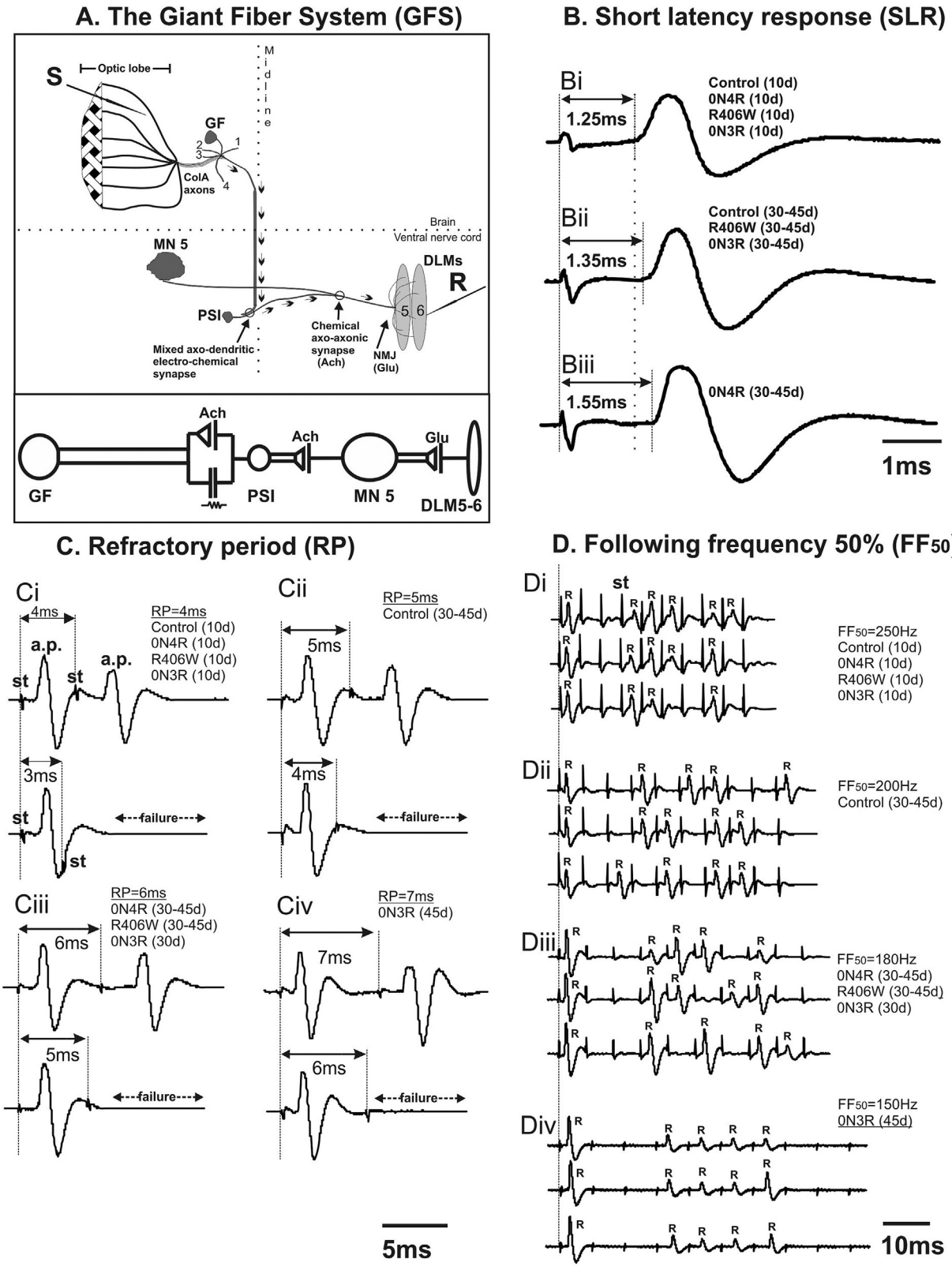

(caption on next page)

(the Short Latency Response-SLR) is a measure of GFS axonal conduction velocity and synaptic delay. It measures the interval between GF action potential generation, signal transmission via the interneurons and the onset of the rising phase of the action potential in the muscle (marked by dotted lines in Fig. 1Bi and 2Bi). The Refractory Period (RP) reflects the reliability of the circuit responsiveness during twin-pulse stimulation and measures the minimum interstimulus interval (ITI) that permits successful response for each stimulus. This is demonstrated in Fig. 1Ci, where a 4 msec ITI between stimuli (st) yields consecutive responses for all genotypes tested. However, reducing the ITI to 3 msec

Fig. 1. The Giant Fiber System (GFS)-DLM5/6 pathway and its functional parameters measured. A. The tri-neuronal part of the GFS consists of the giant fiber (GF) interneuron presynaptic to the peripherally synapsing interneuron (PSI), which in turn synapses with the axon of the motor neuron 5 (MN5). The MN5 axon innervates the dorsal longitudinal muscles 5 and 6 (DLM5–6) (also see the inset below). B-D. Representative traces are shown for 10, 30 and 45 day-old control flies and flies expressing 0N4R, 0N3R and the R406W mutant hTau specifically in GFS neurons (*OK307-Gal4*) Re: recording site, Ach: Acetylcholine, Glu: Glutamate, R: Response, F: Failure, d: day. B. Muscle action potentials recorded by DLM 5 or 6 after GF stimulation. The SLR is indicated by dotted lines as the interval between the action potential generating stimulus artifact (st) and the onset of the rising phase of the muscle action potential (signal transmission through 3 neurons to the muscle, arrows in A). C. The RP is the minimum interstimulus interval (in ms) for which a double response occurred. (Ci) When the two electrical stimuli were delivered with a delay of 4 ms both stimuli generated sequential action potentials in the GF-PSI-MN5-DLM5,6 pathway (upper panel), but the delay was decreased to 3 ms, the second stimulus did not yield an action (lower panel). D. The FF_{50} is the following frequency at which 3 trains of 10 stimuli produce 50% successful responses (15 responses out of 30 stimuli). For example, in (Di), 10 stimuli (st) are followed by 6 responses (R) in the upper trace, by 5 responses in the middle trace and by 4 responses in the lower trace. Thus a total of 30 stimuli produced 15 responses.

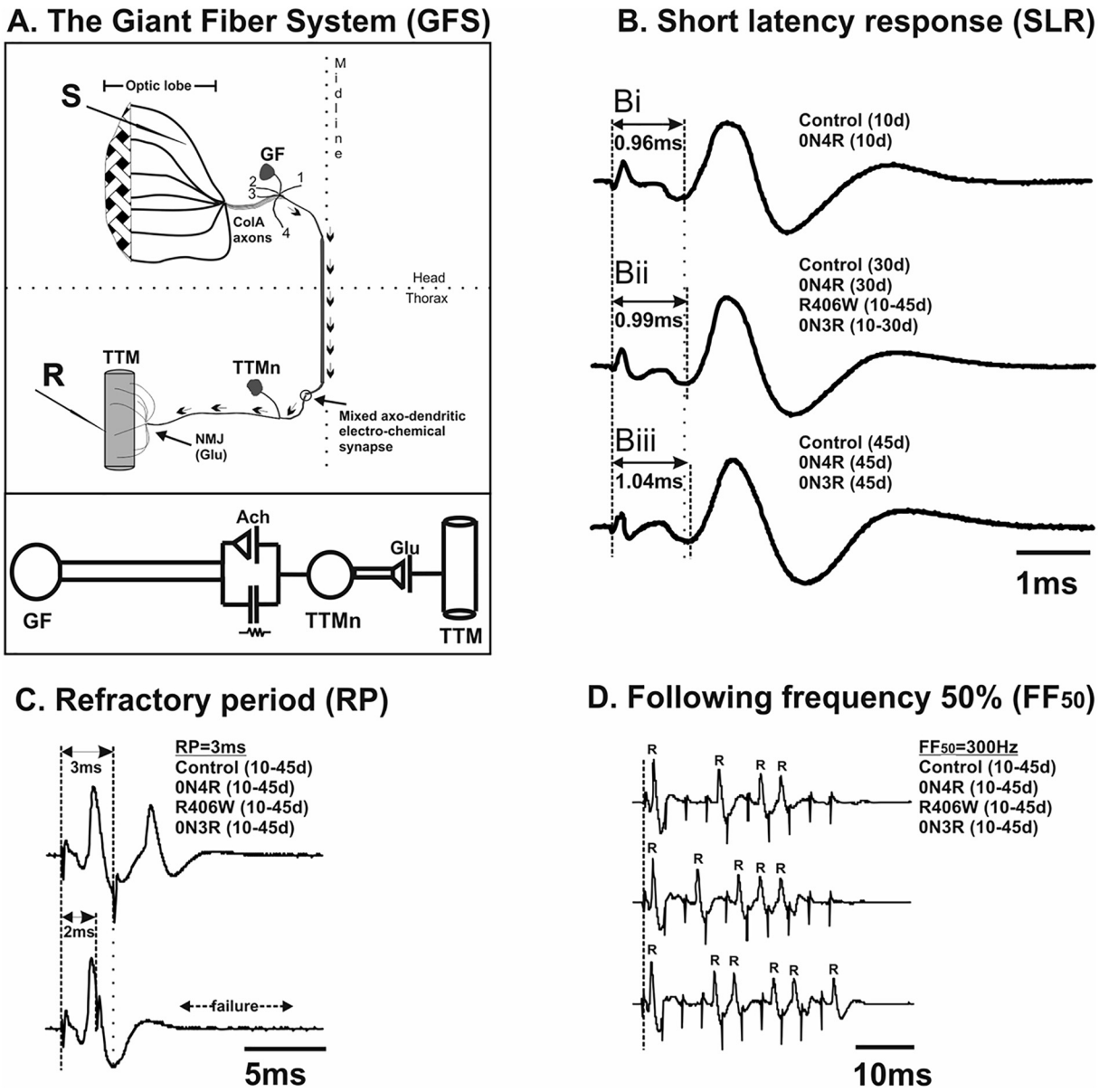

Fig. 2. The Giant Fiber System (GFS)-TTM pathway and its functional parameters measured. A. The bi-neuronal part of the GFS used herein consists of the giant fiber (GF) interneuron presynaptic to the tergotrochanteral muscle motor neuron (TTMn), which outputs directly via glutamatergic synapses onto the tergotrochanteral (jump) muscle (TTM). B-D. Representative traces are shown for 10, 30 and 45 day-old control flies and flies expressing 0N4R, 0N3R and the R406W mutant hTau specifically in GFS neurons (*OK307-Gal4*) Re: recording site, Ach: Acetylcholine, Glu: Glutamate, R: Response, F: Failure, d: day. B. Muscle action potentials recorded in the TTM after GF stimulation. The SLR is indicated by dotted lines as the interval between the action potential generating stimulus artifact (st) and the onset of the rising phase of the muscle action potential. C. The RP is the minimum interstimulus interval (in ms) for which a double response occurred as explained in the legend of Fig. 1 (dotted lines). D. The FF_{50} is the following frequency at which 3 trains of 10 stimuli each produce 50% successful responses (15 responses out of 30 stimuli, as explained in the legend of Fig. 1 (dotted lines).

eliminates the response to the second stimulus and therefore the RP is 4 msec in the DLM branch, while for the same reasons it is 3 msec for the TTM (Fig. 2C). Another measure of system reliability under high frequency transmission is reflected by the frequency at which 3 trains of 10 stimuli each would produce 50% (15 out of 30 stimuli) successful responses and is termed following frequency 50% (FF_{50}). Thus, at 250 Hz stimulation, a total of 30 stimuli produced 15 responses, which is the FF_{50} for the DLM branch, while it is also 15 but at the stimulation rate of 300 Hz for the TTM branch (Fig. 2D). The FF_{50} is higher in the GF-TTM pathway because the signal from GF to the TTM motoneuron is transmitted predominantly via electrical synapses. In the GF-DLM pathway the signal from the GF to PSI is transmitted also via electrical synapses but then the cholinergic synapse between the PSI and the DLM (1-5) motoneurons (in our case MN5 motoneuron) apparently limits transmission capability. Note that glutamatergic Neuromuscular Junction (NMJ) for both pathways can follow above 400 Hz repetitive stimulation.

3.1. 3R and 4R Tau accumulation affect distinct GFS functional parameters

To determine whether accumulation of the 0N4R, 0N3R wild type and the mutant ($0N4R^{R406W}$, or R406W for short), human Tau isoforms affect the functionality of the GFS in an age-dependent manner the SLR, RP and FF_{50} were assessed in control and hTau-expressing flies at 10, 30 and 45 days of age. Initially the effects of hTau proteins were assessed under OK307Gal4, driving their expression throughout the GFS and recorded from DLM5-6 (Fig. 3 insert). To simplify the analysis and use the most appropriate and conservative control, we initially compared the performance of OK307/+ controls with the three transgene heterozygotes (Table 1). For 10 day-old animals significant differences in SLR, RP or FF_{50} were not uncovered. However, for 30 day-old transgene heterozygotes, significant performance improvements were observed for all three measures. Similarly, significantly better FF_{50} performance was observed for 45-day old R406W and 0N3R heterozygotes compared to OK307/+ (Table 1). Because we hypothesized that hTau expression will result in deficits in GFS function, we used the OK307/+ heterozygotes as the most conservative control in all subsequent experiments to avoid false positives by comparing to significantly better performing controls.

As demonstrated in Fig. 1Bi and quantified in Fig. 3A, significant differences in SLR were not uncovered among 10 day-old OK307 controls and hTau transgene-expressing flies with mean response latencies around 1.25 msec. Latencies were increased in older hTau-expressing flies (Fig 1Bii, iii) and quantification demonstrated highly significant differences between controls, and 30 and 45-day old 0N4R-expressing animals (Fig. 3A). Interestingly, however, SLRs were not altered in similarly aged R406W and 0N3R- expressing animals relative to controls (Fig. 3A), strongly suggesting that the effect is specific to the 0N4R hTau isoform. The increased SLR in 0N4R-expressing animals likely underlies increases either in the axonal conduction time and/or synaptic delay as the signal progresses via the multi-synaptic GFS to DLM5–6.

The refractory period (RP) was around 4 msec for 10 day-old controls and hTau expressing animals (Fig. 1Ci) and was not significantly different among genotypes (Fig. 3B). Although the RP increased to 5 msec for 30 and 45-day old control and experimental animals it was significantly different from controls only for 45 day-old 0N3R-expressing flies where RP was increased to 7 msec (Fig. 1Civ and Fig. 3B). Finally, the functional reliability of the GFS measured by the FF_{50} was reduced as controls and experimental animals aged from 10 to 45 day-old (Fig. 1Di-iv). At 45 days of age, the difference with the OK307/+ controls was significant only for 0N3R-expressing animals again (Fig. 3C). Collectively, the significant changes in RP and FF_{50} of 0N3R expressing GFS neurons indicate a specific increase in failure rate upon high-frequency synaptic transmission and may reflect synaptic transmission impairment likely caused by axonal transport malfunction.

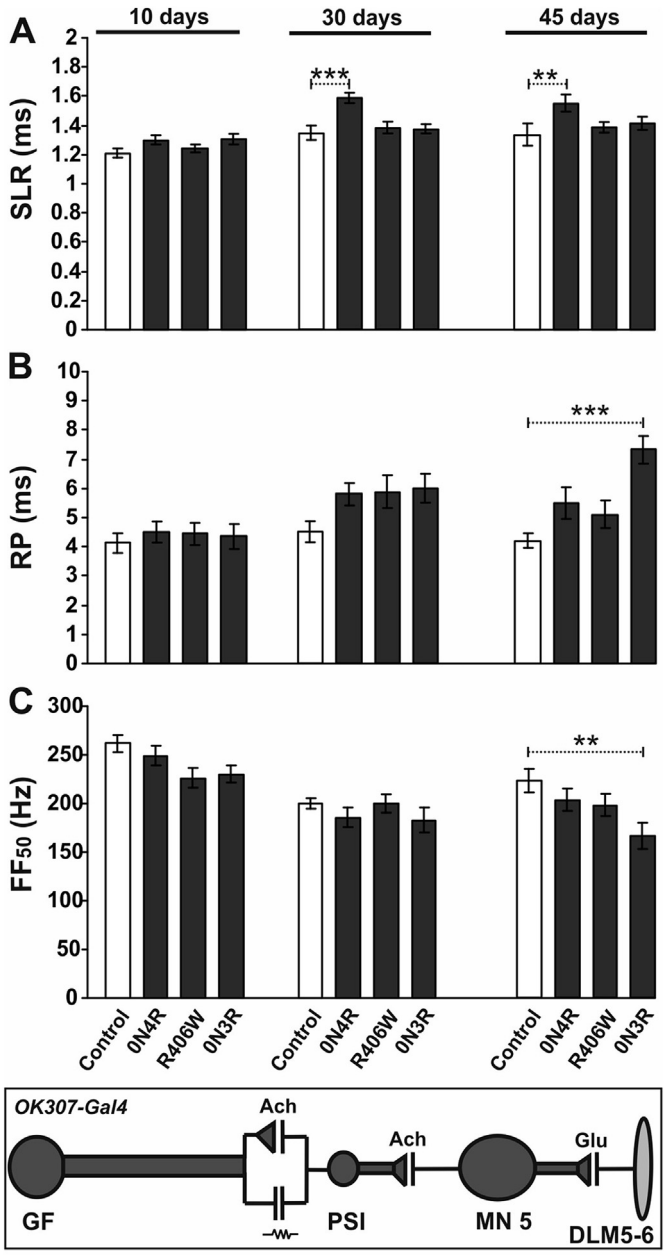

Fig. 3. Targeted hTau expression throughout the GFS under OK307 Gal4. Inset: GF, PSI and MN5 neurons in grey. Recordings from all genotypes for each of the three age cohorts were performed in the same session(s). The means ± SEM are plotted for each parameter indicated. A, The SLR was significantly higher in 30–45 day-old flies expressing 0N4R compared to control flies of equivalent ages, but differences were not uncovered for young flies (10 days-old) of all genotypes. B-C. 0N3R expression precipitates a statistically significant increase in RP (B) and decrease in FF_{50} (C) only in 45 days-old flies. By contrast, 0N4R or R406W expression had no detectable effect (A-C). n = 6–12. Asterisks indicate p values from one-way ANOVA with posthoc Dunnett's tests (**$p < 0.01$, ***$p < 0.001$).

Significantly these deficits were absent in R406W and 0N4R-expressing animals, indicating that they are specifically mediated by the 0N3R hTau isoform.

An additional significant point raised by these results is the apparent lack of effects in any of the parameters measured for the R406W mutant 0N4R isoform, irrespective of the age of the animals (Fig. 3A, B, C). A trivial explanation for this difference would be that the R406W mutant isoform is expressed at lower levels than its parental 0N4R wild type isoform. To address this, we performed western blots to quantify

Table 1
Electrophysiological properties of 10–45 day-old (shading) driver and transgene heterozygotes. The performance of transgene heterozygotes was compared to that of driver heterozygotes for each age group. Significant differences are in bold.

Genotype/age	SLR			RP			FF50		
	Mean	SEM	p	Mean	SEM	p	Mean	SEM	p
OK307/+ 10d	1.21	0.03376	–	4.125	0.3504	–	261.7	10.14	–
0N4R/+ 10d	1.154	0.02645	0.5299	3.125	0.125	0.0163	264.3	9.476	0.9963
R406W/+ 10d	1.213	0.0418	0.9997	3.5	0.2687	0.1485	264.3	9.476	0.9963
0N3R/+ 10d	1.252	0.02606	0.6854	3	0.0	0.005	263.8	11.33	0.9979
OK307/+ 30d	1.346	0.04701	–	4.5	0.378	–	200	5.976	–
0N4R/+ 30d	1.333	0.01947	0.9855	3.375	0.183	**0.0017**	248.8	11.72	**0.0023**
R406W/+ 30d	1.161	0.03401	**0.0013**	3	0.0	< **0.0001**	301.1	7.896	< **0.0001**
0N3R/+ 30d	1.227	0.02569	**0.0315**	3.1	0.1	< **0.0001**	283	8.95	< **0.0001**
OK307/+ 45d	1.337	0.04159	–	4.2	0.1333	–	222.5	12.21	–
0N4R/+ 45d	1.307	0.03762	0.8566	3.75	0.491	0.5	251.4	18.7	0.2369
R406W/+ 45d	1.267	0.02204	0.3537	3.143	0.1429	0.0291	290	9.258	**0.0014**
0N3R/+ 45d	1.307	0.02386	0.8378	3.417	0.193	0.0713	282	6.633	**0.002**

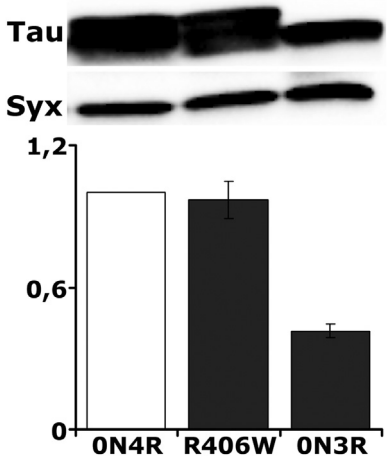

Fig. 4. Accumulation profile of hTau isoforms. Single flies (head + thorax) expressing wt Tau or the FTDP-17 associated mutant R406W driven by OK307 driver were subjected to western blotting with 5A6 antibody. Total Tau levels were normalized to the Syntaxin level (Syx) and shown as ratios of their means ± SEM relative to that in flies expressing 0N4R ($n = 5$). Only 0N3R Tau levels were significantly different (Dunnett's test $p < 0.001$).

the expression level of the three hTau transgenes in OK307Gal4-marked neurons. As shown in Fig. 4, the levels of 0N4R and R406W within these neurons were equivalent as reported before for their pan-neuronal expression (Kosmidis et al., 2010; Papanikolopoulou et al., 2018). The broad band on the blot actually represents partially or incompletely phosphorylated hTau within the GFS as previously reported for other Drosophila neuronal types (Grammenoudi et al., 2006). These results demonstrate that although expressed equivalently to 0N4R, the R406W mutant of the 0N4R isoform does not affect GFS function. In addition, these results provide strong support for the notion that the observed deficits are not a mere consequence of exogenous hTau expression in the GFS, but rather the specific isoforms therein. Interestingly however, the levels of the smaller 0N3R were significantly reduced relative to 0N4R, unlike what has been reported for pan-neuronal expression (Kosmidis et al., 2010; Sealey et al., 2017). Nevertheless, although at relative reduced levels, accumulation of the 0N3R isoform increased the GFS failure rate upon demanding stimulation in an age-dependent manner. Failure rate was not affected by the 0N4R and R406W isoforms even though present at higher levels, suggesting that the RP and FF_{50} deficits are consequent specifically of 0N3R accumulation. The reduced levels of 0N3R relative to 0N4R do not allow comparisons regarding the specificity of the SLR deficits between these two isoforms.

3.2. hTau expression does not alter electrical synaptic transmission and axonal spike propagation in the GFS

The pathway to DLM5/6 activation involves mixed electro-chemical connections from the GF with its postsynaptic PSI (Fig. 1), whereas the pathway to TTM also involves mixed electro-chemical connections from the GF with its postsynaptic TTMn (Fig. 2). Importantly, signal transmission is mostly mediated by the electrical synapse in both cases (Figs. 3, 5 bottom). Disruption of these gap junctions by mutations or knockdown of *shakB* at the GF/TTM synapse increases the SLR between GF and TTM and at the GF/PSI synapse effectively blocks transmission between GF and DLMs (Allen and Murphey, 2007; Pézier et al., 2016). Therefore, to determine whether the SLR, RP and FF_{50} defects uncovered above are due to hTau-induced dysfunction of the electrical or the cholinergic synapses from the GF to MN5 we took two complementary approaches.

Initially we recorded from the PSI-independent GF-TTM pathway in controls and flies expressing the 3 hTau isoforms. Because the GF is connected to TTMn via mixed synapses (Fig. 2A bottom, Fig. 5 bottom), recording from the muscle provides direct functional interrogation of the effects of hTau on the electrical synapse between GF and TTMn and the neuromuscular junction between TTMn and TTM. Significant differences in transgene heterozygotes within each age cohort were not uncovered for SLR, RP and FF_{50} recordings from the TTM (Table 2). Significantly, recording from the TTM did not reveal any differences in the three electrophysiological parameters for hTau-expressing animals and for any age cohort (Fig. 5A–C). The signal, upon direct stimulation of the GF neuron, passes via electrical synapses to TTMn, and via glutamatergic synapses to the muscle (Fig. 5 bottom). Therefore, the results indicate that hTau isoforms do not interrupt assembly, homeostatic maintenance and functionality of Gap-junctions in the dendrites of the TTM motoneuron, or its axon transmitting the signal to the TTM.

To address this question more directly, the effects of the three hTau proteins on the functionality of the GF interneurons of the GFS were assessed. GF interneurons possess the longest and largest axons in Drosophila (Allen et al., 2006), and hTau were selectively expressed therein under the GF-split-Gal4 driver (see Material and Methods for genotype). Although GF interneurons make mixed electro-chemical connections with their postsynaptic PSIs, signal transmission between them is mediated through the electrical synapse (Fig. 6 bottom). Therefore, changes in SLR, RP or FF_{50} upon specific hTau transgene expression in GF interneurons, would be likely due to deregulation or impairment of physiological mechanisms that ensure fast and reliable spike propagation in GF axons and signal transmission via the GF/PSI electrical synapse.

Importantly, significant differences in SLR, RP or FF_{50} were not detected within the three age cohorts of controls and animals

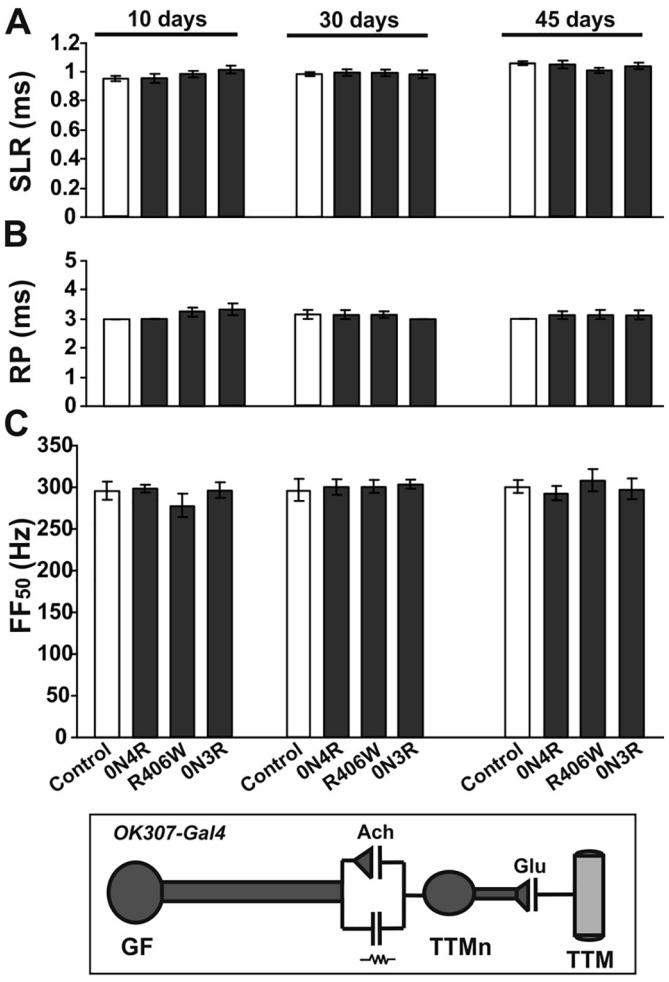

Fig. 5. Recording from the TTM does not reveal defects in flies expressing hTau in the GFS. Inset: GF, TTMn and TTM neurons in grey. Recordings from all genotypes for each of the three age cohorts were performed in the same session (s). The means ± SEM are plotted for each parameter indicated. ANOVA did not indicate differences in the performance of controls (open bars) and experimental animals for any of the three parameters assayed (SLR, RP and FF_{50}) and any age cohort.

expressing hTau in GF interneurons (Fig. 6A–C). Split-Gal4 drivers are thought to be expressed at lower levels, but the trivial explanation that we failed to see an effect due to lower hTau levels is not consistent with by the lack of an effect at the GF/TTMn electrical synapse (Fig. 5A–C), where the levels of the transgenic proteins are adequate to yield deficits (Fig. 3A–C). In contrast, the collective results from hTau expression in the GFS and recording from the DLM (Fig. 3) and the TTM (Fig. 5), combined with the results when expression is limited to the GF are consistent with another explanation. That the age-dependent SLR increase upon 0N4R expression and the deficits in RP and FF_{50} in 0N3R-expressing animals are unlikely due to defects in action potential propagation along the GF and impaired electrical signal transmission. Rather, these deficits are likely the consequences of impairments in the central cholinergic PSI/MN5 and/or the peripheral MN5/DLM5–6 glutamatergic synapses.

3.3. hTau expression does not alter glutamatergic synaptic transmission

To strengthen one of these two possibilities, the hTau transgenes were expressed specifically in the motor neuron MN5 at the exclusion of the cholinergic interneurons (GF and PSI), under c380-Gal4; Cha-Gal80 (Fig. 7, bottom). Since recordings were made from the DLM5-6, this genetic arrangement interrogates specifically motoneuron action potential propagation and the functionality of the glutamatergic neuromuscular synapse.

Expression of hTau isoforms in MN5 did not alter the latency and reliability parameters in any of the age cohorts (Fig. 7A–C). Hence, MN5 action potential generation and propagation to its terminals and transmission through the glutamatergic neuromuscular synapse to DLM5–6 muscles is not altered by the expression of hTau transgenes. In summary then, expression of hTau transgenes specifically in the GF (Fig. 6), or MN5 (Fig. 5) compartments did not phenocopy the electrophysiological deficits precipitated by their expression in the entire GFS (Fig. 3). It follows then that the age-dependent synaptic delay upon 0N4R expression and the increased failures under demanding stimulation upon 0N3R accumulation, derive from aberrant cholinergic transmission at the PSI/MN5 synapse. Specifically, the locus of the defect appears limited to the presynaptic region of the PSI/MN5 synapse, because hTau expression in the postsynaptic MN5 did not have any effects. It is significant that presynaptic function is differentially compromised by 0N4R and 0N3R hTau in a cholinergic synapse because it suggests specific involvement in neurotransmitter release or calcium mediated exocytosis mechanisms by these wild type isoforms and not the mutant R406W.

3.4. Age-specific effects of hTau isoforms on GFS properties

Although we made all GFS performance comparisons within each age cohort, we nevertheless noticed an age-specific performance deterioration for particular genotypes that was absent from similarly aged controls. These differences per parameter are quantified as the

Table 2
Electrophysiological properties of 10–45 day-old (shading) driver and transgene heterozygotes. The performance of transgene heterozygotes was compared to that of driver heterozygotes for each age group. No significant differences were found. n.a. = non applicable because samples all have a standard error of zero.

Genotype/age	SLR			RP			FF50		
	Mean	SEM	p	Mean	SEM	p	Mean	SEM	p
OK307/+ 10d	0.947	0.01643	–	3.000	0.0	–	295.7	10.88	–
0N4R/+ 10d	0.979	0.03041	0.5370	3.000	0.0	n.a.	302.9	7.143	0.9116
R406W/+ 10d	0.980	0.00794	0.5032	3.000	0.0	n.a.	317.1	9.184	0.2828
0N3R/+ 10d	1.004	0.01822	0.1240	3.000	0.0	n.a.	284.3	10.43	0.7327
OK307/+ 30d	0.987	0.01499	–	3.143	0.1429	–	295.7	12.88	–
0N4R/+ 30d	0.978	0.01816	0.9574	3.125	0.1250	0.9994	305.7	11.72	0.8833
R406W/+ 30d	0.987	0.01061	> 0.9999	3.143	0.1429	> 0.9999	311.3	9.531	0.6651
0N3R/+ 30d	1.011	0.01135	0.5116	3.111	0.1111	0.9961	297.1	13.04	0.9995
OK307/+ 45d	1.049	0.01279	–	3.000	0.0	–	300.0	8.452	–
0N4R/+ 45d	1.034	0.02526	0.9373	3.000	0.0	n.a.	315.7	3.689	0.4318
R406W/+ 45d	1.060	0.03022	0.9770	3.000	0.0	n.a.	324.3	6.117	0.1328
0N3R/+ 45d	1.031	0.02853	0.9060	3.000	0.0	n.a.	324.3	12.88	0.1328

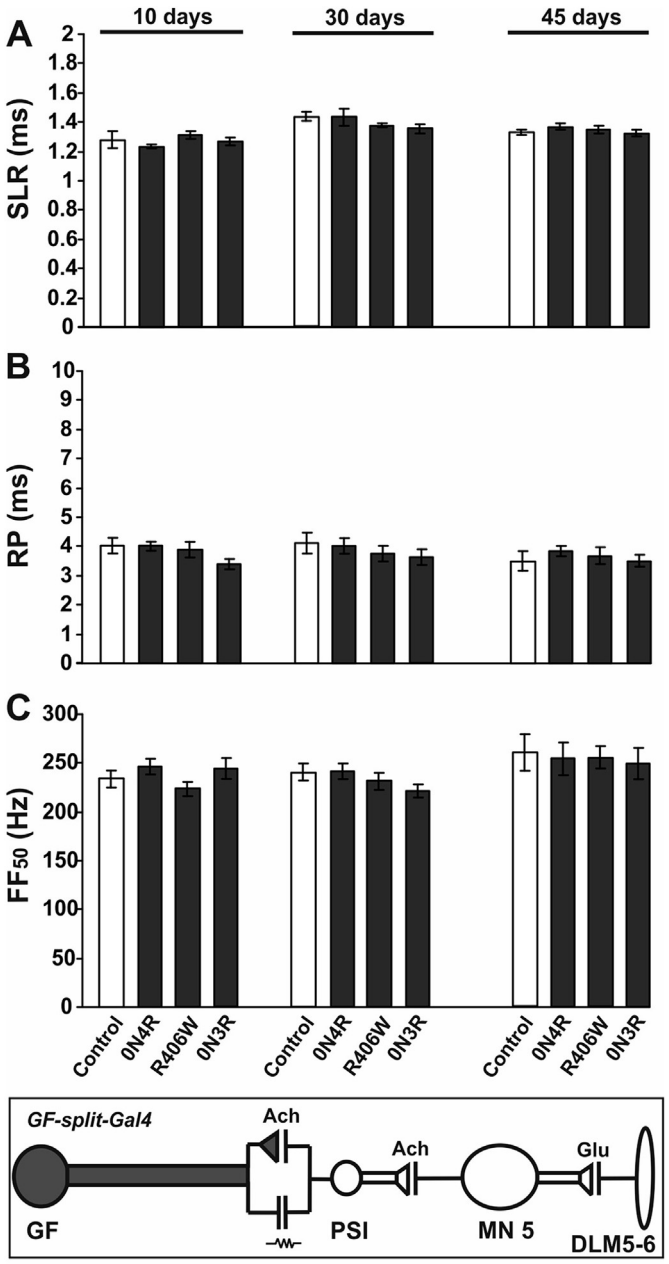

Fig. 6. Targeted hTau expression in the GF interneuron. Targeted expression of 0N4R, 0N3R and 0N4R^{R406W} hTau exclusively in the GF interneuron, under GF-split-Gal4 (inset: GF in grey) did not yield detectable differences from controls for any age cohort in SLR (A), the RP (B) and the FF_{50} (C). The means ± SEM are plotted for each parameter indicated. n = 5–10.

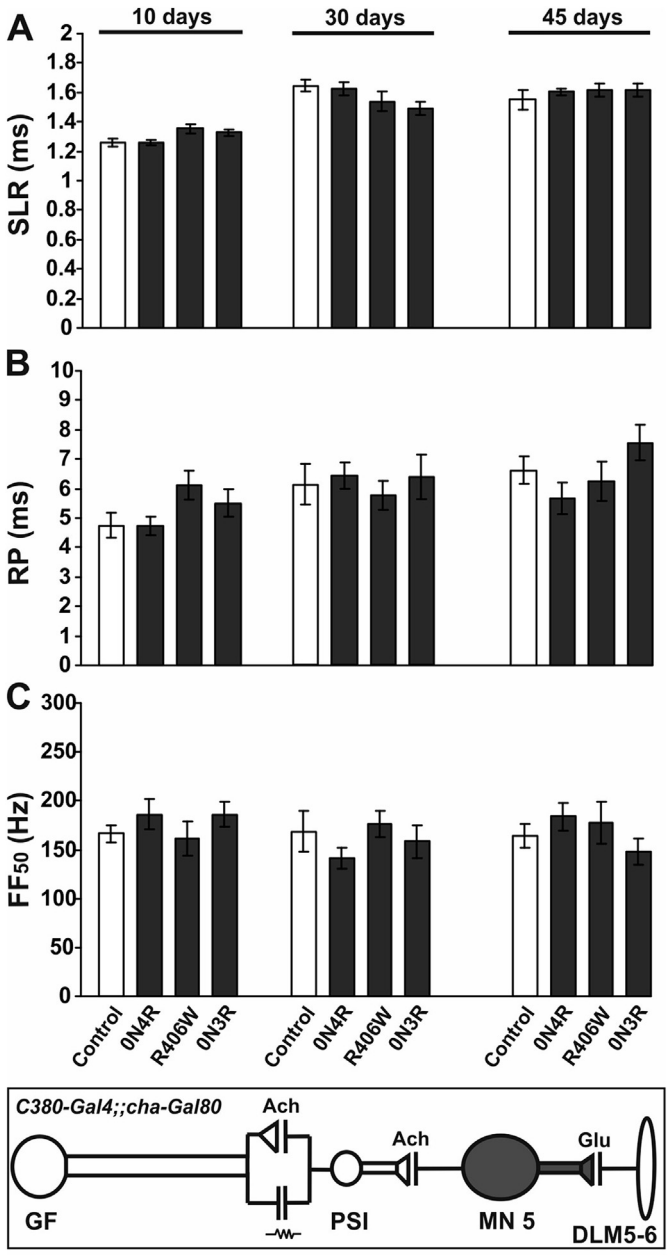

Fig. 7. Targeted hTau expression in the MN5 motor neuron. Targeted expression of 0N4R, 0N3R and 0N4R^{R406W} hTau exclusively in the MN5 neuron GF interneuron, under GF-split-Gal4 (*C380-Gal4; cha-Gal80*) (inset: MN5 in grey), did not yield detectable differences from controls for any age cohort in SLR (A), the RP (B) and the FF_{50} (C) The means ± SEM are plotted for each parameter indicated. *n* = 7–10.

difference in mean performance between 10 day-old control and experimental animals with 30 and 45-day old animals of the same genotype (Fig. 8A). Whereas controls do not show an age-dependent decline in SLR, both 0N4R and R406W-expressing flies at 30 and 45 days present significantly increased latencies in comparison to their 10 day-old cohort (Fig. 8A, B).

Importantly, whereas 0N3R-expressing animals did not present an age-dependent SLR decline, they alone exhibited significant RP differences in 30 and 45-day old animals compared to the 10-day old counterparts (Fig. 8A, C). In contrast, controls presented significant age-dependent decline in FF_{50}. Hence, it is difficult to conclude that this increased failure rate is specific to the experimental animals. Interestingly however, age-dependent alterations in FF_{50} performance were not detectable for R406W-expressing flies (Fig. 8A). It is also noteworthy that significant differences were not apparent in any of the parameters tested between 30 day and 45 day-old flies and for any of the genotypes. This is consistent with the observed significant 50% decline in the levels of all hTau isoforms between day 30 and 45 expressed under the OK307 driver (Fig. 8C) and may reflect age-dependent decrease in OK307Gal4 expression. Nevertheless the results indicate that the damage to the cholinergic PSI/MN-5 synapse incurred by day 30 is maintained even when hTau levels decline. This may reflect that the synaptic damage by day 30 is irreversible, or alternatively, the age-dependent 0N4R, R406W and 0N3R-mediated SLR and RP impairments respectively do not depend on the levels, but rather the particular hTau isoform present at the PSI interneuron. Differentiation between these two possibilities is currently under investigation.

A

Driver	Parameter	Genotype	10d vs 30d	10d vs 45d	30d vs 45d
OK307	SLR	Control	ns (0.0849)	ns (0.1022)	ns (0,9869)
OK307	SLR	0N4R	**0.0002**	**0.0011**	ns (0.8344)
OK307	SLR	R406W	**0.0172**	**0.0091**	ns (0.9880)
OK307	SLR	0N3R	ns (0.4697)	ns (0.1353)	ns (0.7284)
OK307	RP	Control	ns (0.6542)	ns (0.9810)	ns (0.7383)
OK307	RP	0N4R	ns (0.1124)	ns (0.2621)	ns (0.8810)
OK307	RP	R406W	ns (0.1060)	ns (0.5704)	ns (0.5019)
OK307	RP	0N3R	**0.0395**	**0.0003**	ns (0.1302)
OK307	FF50	Control	**0.0011**	**0.0341**	ns (0.2338)
OK307	FF50	0N4R	**0.0015**	**0.0178**	ns (0.5086)
OK307	FF50	R406W	ns (0.2149)	ns (0.1522)	ns (0.9875)
OK307	FF50	0N3R	**0.0209**	**0.0016**	ns (0.5602)

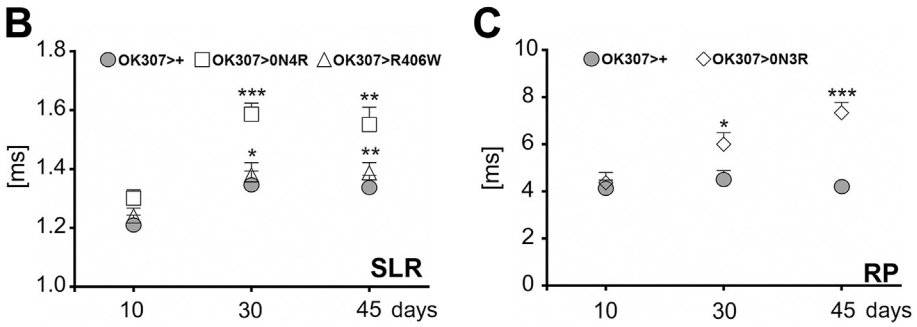

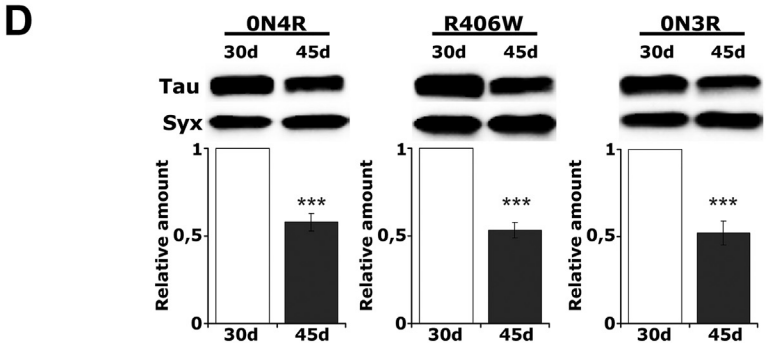

Fig. 8. Age dependent decline in GFS latency and fidelity by specific hTau isoforms. A. Comparison of the mean ± SEM SLR, RP and FF_{50} for the three age cohorts expressing the indicated hTau wild type and mutant isoform. The mean performances per parameter for the 30 and 45 day-old cohorts were compared to those of 10 day-old animals of the same genotype. Significant differences are in bold, while non-significant differences are indicated by ns and the probability values are given within parentheses. B. Age dependent increases in SLR specifically for 0N4R and R406W. The significance asterisks refer to the performance differences between the 10 day-old flies and the 30 day and 45 day-old age cohorts of the same genotype. C. Age dependent increases in RP specifically for 0N3R. The significance asterisks refer to the performance differences between the 10 day-old flies and the 30 day and 45 day-old age cohorts of the same genotype. D. Age-dependent expression decline of hTau isoforms in the GFS. Lysates from the head + thorax of flies expressing under OK307Gal4 the indicated Tau transgenes were subjected to western blotting. Flies were kept at 25C for 30 and 45 days respectively. Significant reduction (Dunnett's, $p < 0{,}0001$ $n = 4$) in Tau levels at 45d compared to 30d was revealed for all hTau isoforms with the total Tau 5A6 antibody while Syntaxin (Syx) was used as a loading control. For the quantification shown below each representative blot, Tau levels were normalized to Syx and shown as a ratio of their means ± S.E.M. relative to their respective levels in fly heads expressing Tau at 30d, which was set to 1.

In animals expressing the transgenes in the GF or MN5, significant age specific decline in the three measured parameters was not observed, except for the generalized SLR impairment in SLR in controls and all experimental animals under the MN5-specific Gal4 driver (Table 3). This strengthens the conclusion of an age-dependent hTau isoform-specific decline in specific functional properties at the presynaptic side of the cholinergic synapse to MN5.

4. Discussion

Drosophila has been used to model many aspects of Tauopathies and Alzheimer's disease ranging from neurodegeneration to learning and memory deficits and through its genetic facility has been used to reveal dysregulated molecular mechanisms potentially underlying these diverse pathologies (Fernandez-Funez et al., 2015; Papanikolopoulou and Skoulakis, 2011; Sun and Chen, 2015). However, except for the larval neuromuscular junction (Chee et al., 2005), little has been done to probe the effects of Tau accumulation on the electrophysiological properties of Drosophila CNS neurons. This is particularly apparent when it comes to properties of neuro-neuronal synapses of adult Drosophila when defects in learning and memory, typically associated with the major Tauopathies (Lee et al., 2001), are investigated (Kosmidis et al., 2010; Papanikolopoulou and Skoulakis, 2015; Sealey et al., 2017).

Although accumulation of both 0N3R and 0N4R wild type hTau isoforms caused functional deficits, their effects on GFS conduction properties were differential. 0N3R isoform accumulation increased failures under high demand, whereas 0N4R compromised conduction and response speed. This is in accord with recent results suggesting that even though both isoforms compromised axonal transport in larval motor neurons, the defects were stronger for 0N3R (Sealey et al., 2017). This in turn may underlie the increase in GFS failures under high frequency stimulation, represented by the increased refractory period and decreased FF_{50}. These results encourage a systematic investigation of all 6 human Tau isoforms in these GFS functional parameters in an age-dependent manner.

Importantly, accumulation of the R406W mutated 0N4R form, which is associated with FTDP-17 (Goedert, 2005; Goedert et al., 1998) did not precipitate the strong effects its wild type cognate (Fig. 2), typically involved in AD (Lee et al., 2001), did. Because R406W is just as toxic as 0N4R (Khurana et al., 2006; Kosmidis et al., 2010; Reed et al., 2001), this result suggests that the mutation ameliorates the effects of 0N4R accumulation on GFS functional physiology. This is consistent with the mild but significant age-dependent SLR effects of the mutant in comparison with those precipitated by 0N4R, indicating that the wild type and the R406W mutant of the 0N4R isoform in fact affect the same GFS functional parameters. This, together with the differential effects of the two wild type isoforms strongly suggest that the compromised GFS functional properties are not mere consequences of exogenous hTau accumulation. Therefore, the differential effects of the 0N3R and 0N4R on GFS physiology suggest that these isoforms likely engage distinct mechanisms required for cholinergic signal transmission and synaptic

Table 3
Age- specific effects of hTau transgene expression in the GF (no shading) and the MN-5 neuron (shaded). The mean SLR, RP and FF_{50} performance of each genotype at 30 days and 45 days is compared to that of the 10 day-old cohort. Significant differences are presented in bold.

Driver	Parameter	Genotype	10d vs 30d	10d vs 45d	30d vs 45d
GF	**SLR**	**Control**	**0.0263**	ns (0.6948)	ns (0.2034)
GF	**SLR**	**0N4R**	**0.0037**	ns (0.0617)	ns (0.4592)
GF	**SLR**	**R406W**	ns (0.2075)	ns (0.5781)	ns (0.6970)
GF	**SLR**	**0N3R**	ns (0.0545)	ns (0.2404)	ns (0.6605)
GF	**RP**	**Control**	ns (0.9655)	ns (0.5715)	ns (0.4218)
GF	**RP**	**0N4R**	ns (> 0.9999)	ns (0.8395)	ns (0.8521)
GF	**RP**	**R406W**	ns (0.9308)	ns (0.8236)	ns (0.9744)
GF	**RP**	**0N3R**	ns (0.6932)	ns (0.9113)	ns (0.9113)
GF	**FF50**	**Control**	ns (0.9927)	ns (0.9910)	ns (0.9691)
GF	**FF50**	**0N4R**	ns (0.0677)	ns (0.9905)	ns (0.0876)
GF	**FF50**	**R406W**	ns (0.8195)	ns (0.7920)	ns (0.9986)
GF	**FF50**	**0N3R**	ns (0.3873)	ns (0.1393)	ns (0.8534)
C380	**SLR**	**Control**	**< 0.0001**	**0.0013**	ns (0.3510)
C380	**SLR**	**0N4R**	**< 0.0001**	**< 0.0001**	ns (0.8763)
C380	**SLR**	**R406W**	**0.0280**	**0.0020**	ns (0.4844)
C380	**SLR**	**0N3R**	**0.0233**	**< 0.0001**	ns (0.0649)
C380	**RP**	**Control**	ns (0.1893)	ns (0.0550)	ns (0.7890)
C380	**RP**	**0N4R**	**0.0364**	ns (0.3399)	ns (0.4338)
C380	**RP**	**R406W**	ns (08784)	ns (0.9856)	ns (07950)
C380	**RP**	**0N3R**	ns (0.5966)	ns (0.0668)	ns (0.3779)
C380	**FF50**	**Control**	ns (0.9927)	ns (0.9910)	ns (0.9691)
C380	**FF50**	**0N4R**	ns (0.0677)	ns (0.9905)	ns (0.0876)
C380	**FF50**	**R406W**	ns (0.8195)	ns (0.7920)	ns (0.9986)
C380	**FF50**	**0N3R**	ns (0.3873)	ns (0.1319)	ns (0.8553)

fidelity, a likely reflection of their functional differences in the human brain as well, indicating potential involvement of hTau isoforms in neurotransmitter release, or calcium mediated exocytosis mechanisms. In agreement with these results, accumulation of soluble Tau in the entorhinal cortex of rTgTauEC transgenic mice, precipitated significant presynaptic deficits (Polydoro et al., 2014).

The effects of hTau accumulation in the GFS recapitulate the age-dependent synaptic dysfunction manifestation in Tauopathies that likely underlies the cognitive deficits in humans and mouse models (Polydoro et al., 2009). Clearly synaptic delay and defects in synaptic reliability appear in an age dependent manner and given that the circuit mediates escape responses in the fly (Allen et al., 2006), it may reflect the compromised climbing and mobility in aged flies expressing these hTau isoforms pan-neuronally (Sealey et al., 2017). Age -dependent decline was also observed for controls and animals expressing 0N4R and 0N3R in MN5 under c380 Gal4 (Table 3), indicating an effect of the Gal4 driver rather than a specific age-dependent sensitivity of that motor neuron.

Finally, despite their differential effects, it is interesting that 0N4R and 0N3R affect the same cholinergic synapse between PSI and MN5, in light of the fact that cholinergic dysfunction has been suggested for Alzheimer's patients and other neurodegenerative diseases (Hamodat et al., 2017; Kolisnyk et al., 2017; Pepeu and Grazia Giovannini, 2017; Simón et al., 2013). This suggests that in general, cholinergic synapses may be particularly sensitive to Tau levels or dysfunction as also suggested by the use of cholinesterase inhibitors as ameliorative for the disease. Because of the genetic facility of the Drosophila model, the experimental system presented herein is likely to help elucidate the mechanism(s) of this sensitivity of the cholinergic synapses in Tauopathies and potentially lead to better ameliorative or therapeutic drugs.

Acknowledgments

DK was funded by the Hellenic Ministry of Education, Research and Religion within the framework of the action “SUPPORT OF POSTDOCTORAL RESEARCHERS” of the OP “Development of Human Resources, Education and Lifelong Learning “, 2014-2020, which is being implemented by the IKY and was co-financed from the European Social Fund and the Greek Public. KP's contribution was made possible through a grant from the Stavros Niarchos Foundation to the Biomedical Sciences Research Center “Alexander Fleming”, as part of the Foundation's initiative to support the Greek research Center ecosystem.

References

Allen, M., Murphey, R., 2007. The chemical component of the mixed GF-TTMn synapse in Drosophila melanogaster uses acetylcholine as its neurotransmitter. Eur. J. Neurosci. 26, 439–445.
Allen, M., et al., 1998. Development of the giant fiber neuron of Drosophila melanogaster. J. Comp. Neurol. 397, 519–531.
Allen, M., et al., 2000. A role for Drosophila Drac1 in neurite outgrowth and synaptogenesis in the giant fiber system. Mol. Cell. Neurosci. 16, 754–765.
Allen, M., et al., 2006. Making an escape: development and function of the Drosophila giant fibre system. Semin. Cell Dev. Biol. 17, 31–41.
Avila, J., et al., 2004. Role of tau protein in both physiological and pathological conditions. Physiol. Rev. 84, 361–384.
Bardai, F., et al., 2018. A conserved cytoskeletal signaling cascade mediates neurotoxicity of FTDP-17 Tau mutations in Vivo. J. Neurosci. 3, 108–119.
Boerner, J., Duch, C., 2010. Average shape standard atlas for the adult Drosophila ventral nerve cord. J. Comp. Neurol. 518 (13), 2437–2455 2437–2455. 518.
Buee, L., et al., 2000. Tau protein isoforms, phosphorylation and role in neurodegenerative disorders. Brain Res. Brain Res. Rev. 33, 95–130.
Chee, F., et al., 2005. Overexpression of tau results in defective synaptic transmission in Drosophila neuromuscular junctions. Neurobiol. Dis. 20, 918–928.
Crowther, D.C., et al., 2006. A Drosophila model of Alzheimer's disease. Methods Enzymol. 412, 234–255.
Delacourte, A., 2005. Tauopathies: recent insights into old diseases. Folia Neuropathol. 43, 244–257.
Duch, C., et al., 2008. Dendrite elongation and dendritic branching are affected separately by different forms of intrinsic motoneuron excitability. J. Neurophysiol. 100, 2525–2536.
Engel, J., Wu, C.-F., 1992. Interactions of membrane excitability mutations affecting potassium and sodium currents in the flight and giant fiber escape systems of Drosophila. J. Comp. Physiol. A. 171, 93–104.
Fernandez-Funez, P., et al., 2015. Modeling the complex pathology of Alzheimer's disease in Drosophila. Exp. Neurol. 274, 58–71.
Goedert, M., 2005. Tau gene mutations and their effects. Mov. Disord. 20 (Suppl. 12), S45–S52.
Goedert, M., et al., 1998. Tau mutations cause frontotemporal dementias. Neuron 21, 955–958.
Gotz, J., et al., 2007. A decade of tau transgenic animal models and beyond. Brain Pathol. 17, 91–103.
Grammenoudi, S., et al., 2006. Cell type-specific processing of human Tau proteins in Drosophila. FEBS Lett. 580, 4602–4606.
Hammond, S., O'Shea, M., 2007. Escape flight initiation in the fly. J. Comp. Physiol. A Neuroethol. Sens. Neural. Behav. Physiol. 193, 471–476.
Hamodat, H., et al., 2017. Cholinesterases in normal and Alzheimer's disease primary olfactory gyrus. Neuropathol. Appl. Neurobiol. 43, 571–583.
Kadas, D., et al., 2012. Constitutive activation of Ca2+/calmodulin-dependent protein kinase II during development impairs central cholinergic transmission in a circuit underlying escape behavior in Drosophila. J. Neurosci. 32, 170–182.
Khurana, V., et al., 2006. TOR-mediated cell-cycle activation causes neurodegeneration in a Drosophila tauopathy model. Curr. Biol. 16, 230–241.
Kolisnyk, B., et al., 2017. Cholinergic Surveillance over Hippocampal RNA Metabolism and Alzheimer's-like Pathology. Cereb. Cortex 27, 3553–3567.
Kosmidis, S., et al., 2010. Differential effects of Tau on the integrity and function of neurons essential for learning in Drosophila. J. Neurosci. 30, 464–477.
Lee, V.M.-Y., et al., 2001. Neurodegenerative tauopathies. Annu. Rev. Neurosci. 24, 1121–1159.
Lee, V.M., et al., 2005. Transgenic animal models of tauopathies. Biochim. Biophys. Acta 1739, 251–259.
Marsh, J.L., Thompson, L.M., 2004. Can flies help humans treat neurodegenerative diseases? BioEssays 26, 485–496.
Mudher, A., et al., 2008. Using Drosophila models to unravel pathogenic mechanisms that underlie neurodegeneration in tauopathies. SEB Exp. Biol. Ser. 60, 25–38.
Papanikolopoulou, K., Skoulakis, E.M., 2011. The power and richness of modelling tauopathies in Drosophila. Mol. Neurobiol. 44, 122–133.
Papanikolopoulou, K., Skoulakis, E.M., 2015. Temporally distinct phosphorylations differentiate Tau-dependent learning deficits and premature mortality in Drosophila. Hum. Mol. Genet. 24, 2065–2077.
Papanikolopoulou, K., et al., 2018. Differential effects of 14-3-3 dimers on Tau phosphorylation, stability and toxicity in vivo. Hum. Mol. Genet. 27, 2244–2261.
Pepeu, G., Grazia Giovannini, M., 2017. The fate of the brain cholinergic neurons in neurodegenerative diseases. Brain Res. 1670, 173–184.
Pézier, A., et al., 2016. Shaking B Mediates Synaptic Coupling between Auditory Sensory Neurons and the Giant Fiber of Drosophila melanogaster. PLoS ONE 11, e0152211.
Polydoro, M., et al., 2009. Age-dependent impairment of cognitive and synaptic function in the htau mouse model of tau pathology. J. Neurosci. 29, 10741–10749.
Polydoro, M., et al., 2014. Soluble pathological tau in the entorhinal cortex leads to

presynaptic deficits in an early Alzheimer's disease model. Acta Neuropathol. 127, 257–270.
Reed, L.A., et al., 2001. Phenotypic correlations in FTDP-17. Neurobiol. Aging 22, 89–107.
Ryglewski, S., D, K., Hutchinson, K., Schuetzler, N., Vonhoff, F., Duch, C., 2014. Dendrites are dispensable for basic motoneuron function but essential for fine tuning of behavior. Proc. Natl. Acad. Sci. U. S. A. 111, 18049–18054.
Sang, T.K., Jackson, G.R., 2005. Drosophila models of neurodegenerative disease. NeuroRx 2, 438–446.
Sanyal, S., R, N., Consoulas, C., Ramaswami, M., 2003. Evidence for cell autonomous AP1 function in regulation of Drosophila motor-neuron plasticity. BMC Neurosci. 4, 20.
Sealey, M.A., et al., 2017. Distinct phenotypes of three-repeat and four-repeat human tau in a transgenic model of tauopathy. Neurobiol. Dis. 105, 74–83.
Sergeant, N., et al., 2005. Tau protein as a differential biomarker of tauopathies. Biochim. Biophys. Acta 1739, 179–197.
Simón, D., et al., 2013. The involvement of cholinergic neurons in the spreading of tau pathology. Front. Neurol. 4, 74.
Sotiropoulos, I., et al., 2017. Atypical, non-standard functions of the microtubule associated Tau protein. Acta Neuropathol Commun. 5, 91.
Sun, M., Chen, L., 2015. Studying tauopathies in Drosophila: a fruitful model. Exp. Neurol. 274, 58–71.
Tanouye, M., Wyman, R., 1980. Motor outputs of giant nerve fiber in Drosophila. J. Neurophysiol. 44, 405–421.
Trimarchi, J., Schneiderman, A., 1993. Giant fiber activation of an intrinsic muscle in the mesothoracic leg of Drosophila melanogaster. J. Exp. Biol. 177, 149–167.
von Reyn, C., et al., 2014. A spike-timing mechanism for action selection. Nat. Neurosci. 17, 962–970.
Wittmann, C.W., et al., 2001. Tauopathy in Drosophila: neurodegeneration without neurofibrillary tangles. Science 293, 711–714.